Colloid & Polymer Science Colloid Polym Sci 272:731–739 (1994)

The measurement of dynamic surface tension by the maximum bubble pressure method

V. B. Fainerman[1]), R. Miller[2]*), and P. Joos[3])

[1]) Institute of Technical Ecology, Donetsk, 340017, Ukraine
[2]) Max-Planck-Institut für Kolloid- und Grenzflächenforschung, Berlin-Adlershof, Germany
[3]) Universitaire Instelling Antwerpen, Department Scheikunde, Antwerpen (Wilrijk), Belgium

Abstract: The principle of maximum pressure in a bubble for measurements of dynamic surface tension is realized in a fully automatically operating apparatus. The set-up yields data in the time interval from 1 ms up to several seconds and can be temperature controlled from 5° to 80 °C. Experimental data obtained for different surfactants and gelatine in water and/or water/glycerine mixtures at different temperatures are discussed. A direct comparison with results from oscillating jet and inclined plate experiments shows excellent agreement.

Key words: Maximum bubble pressure method – dynamic surface tension – surfactant solutions – gelatine – temperature effects

1. Introduction

The dynamic surface tension of liquid-gas interfaces is an important physical parameter which characterizes the surface properties and processes which take place at the surface and in the bulk of a liquid. Rehbinder was apparently the first to apply the maximum bubble pressure method for measurements of dynamic surface tension of surfactant solutions [1]. Further developments of this method were described in [2–7]. It was established specifically that the time interval between subsequent bubbles includes surface lifetime and the so-called "dead time" [4]. A considerable contribution to the development of this method was made by Kloubek [8–10]. He derived a simple experimental procedure for the determination of the dead time [10] and gave also an estimation of the effective bubble surface lifetime [9]. The use of electric pressure sensors for the measurement of pressure and bubble formation frequency [5, 11–15] substantially simplified the measurement procedure. Original apparatuses for the measurement of dynamic surface tension by the maximum bubble pressure method were presented in [16, 17] for the region of long lifetime and in [18] for a modified method with two capillaries. Techniques of oscillating bubbles [19, 20] and direct analysis of the bubble shape at constant bubble volume [21] were also developed.

The implementation of maximum bubble pressure method in the region of high bubble formation frequencies is connected with three main problems:

1) the measurement of bubble pressure;
2) the measurement of bubble formation frequency;
3) the estimation of surface lifetime and effective surface age.

The first problem can be solved easily if the system volume, which is connected with the bubble, is big enough in comparison with the volume of the bubble separating from the capillary.

*) To whom correspondence should be addressed

In this case the system pressure is equal to the maximum bubble pressure. The use of an electric pressure transducer for the measurement of bubble formation frequency presumes that pressure oscillations in the measuring system are distinct enough. This condition is fulfilled in systems with comparatively small volumes. As shown by Mysels [15], the determination of maximum bubble pressure values in systems with a small volume can be erroneous. Apart from a high-speed pressure measuring method, also electric [22, 23] and stroboscopic [3, 4, 7–10] methods for detection of the bubble formation frequency were used. To separate the surface lifetime from the total time interval between subsequent bubbles an appoximation of the dead time according to geometric parameters of capillary and bubble volume was derived in [23, 24]. A substantial improvement for the exact determination of surface lifetime and its calculation was done in [25, 26] where a critical point in the experimental curve in co-ordinates "pressure-gas flow rate" was defined. This point corresponds to a change in the flow regime from individual bubble formation to a gas jet regime. The problem of recalculation of bubble surface lifetime to the so-called effective age of the surface (effective adsorption time) was discussed in [25–30].

In the present paper an instrument is described for the measurement of dynamic surface tension based on the principle of maximum pressure in a bubble. In this set-up, available as the commercial device MPT1 from Lauda (Germany), all theoretical and experimental problems are solved. Beside results obtained from studies with this instrument for very different systems, including pure solvents and aqueous surfactant and protein solutions, a comparison with data obtained from other methods is presented.

2. The design and operation of the instrument

A block-scheme of the instrument for the measurement of dynamic surface tension by the maximum bubble pressure method is shown in Fig. 1. The air coming from a microcompressor (1) is purified in a fine gas purification filter (2). Then it flows through a triple-stroke valve (3), realized by a combination of three magnetic valves, to the throttling capillary (4). The air flow rate is measured with the help of an electric transducer (8) according to the pressure difference between the two ends of capillary (4). Thereafter the air enters the removable part (12) of the measuring cell (14). The excess air pressure in the system is measured by an electric sensor (9). In the tube which feeds the air to the measuring cell (14), a sensitive microphone (5) is placed. The measuring cell (14) is equipped with a water jacket which allows a connection with an external thermostat. It has also an outlet pipe (13) to let out the excess air. The removable part (12) of the measuring cell consists of a capillary (15) and two platinum electrodes (16), one of which is immersed into the liquid under study and the second is situated exactly opposite the capillary (15). This electrode is welded into a glass pipe, and only the very end is in contact with the liquid. The removable part of the measuring cell has a cavity which is filled with the liquid to ensure a saturated atmosphere. The electric signals from the gas flow rate sensor (8) and pressure transducer (9), the microphone (5) and electrodes (16) are send to the control block (10), which is connected with a computer (11) via

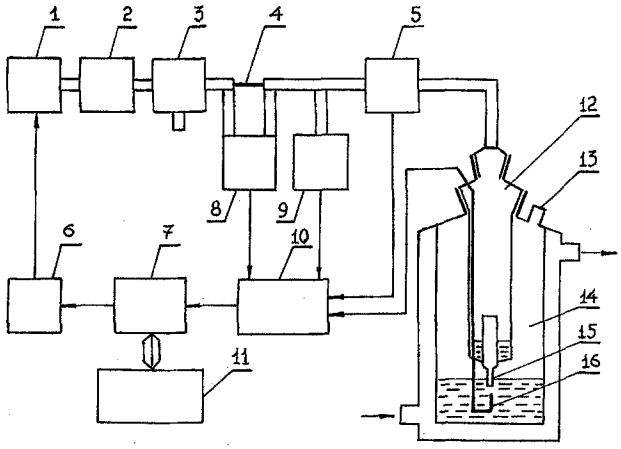

Fig. 1. Block-scheme of the maximum bubble pressure apparatus.
Designations: 1 – micro-compressor; 2 – fine air purification filter; 3 – three-stroke valve (stopcock, or actually a combination of three magnetic valves); 4 – throttling capillary; 5 – microphone; 6 – micro-compressor control block unit; 7 – analog-digital converter; 8 – gas flow rate sensor; 9 – pressure sensor (transducer); 10 – measuring block; 11 – IBM-compatible computer; 12 – separable part of the measuring cell; 13 – air outlet connection pipe; 14 – measuring cell; 15 – capillary; 16 – electrode system

an analog-digital converter (7). The operational control of the compressor (1) is also organized by the computer (11) via block (6).

In the present instrument two independent systems for measuring the bubble formation frequency are implemented: the acoustic system is based on a microphone (5) and the electric one operates with platinum electrodes (16). While the electric system can be used only for electro-conductive liquids, the acoustic one is applicable to any liquids. A sketch of a bubble at the tip of a capillary immersed into the liquid is shown in Fig. 2. At the very beginning the bubble radius r_0 is bigger than the capillary radius r. After the time τ, which represents the so-called surface lifetime, the bubble radius decreases and becomes equal to the capillary radius. In systems with a relatively small volume in this moment the pressure will reach its maximum value in the measuring system. Thereafter, the bubble radius decreases again and the bubble grows quickly. When the growing bubble reaches the electrode oppositely located to the capillary, a change in the electric conductivity of the electrode system 16 (Fig. 1) results and can be registered by the control block (10). After touching the electrode the bubble loses its stability and symmetry and emerges after separation from the capillary. The gas cavity connecting the bubble with the capillary collapses and the sound wave accompanying this phenomenon is registered by the microphone (5). The time interval of the fast bubble growth (counting from hemisphere of the bubble up to the interval of cavity collapse) is called dead time. Thus, we have $\tau_d + \tau = \tau_b$, where τ_b is the time interval between subsequent bubbles. In the present instrument very thin glass capillaries with a smooth and straight surface were used having radii between 0.07 and 0.08 mm and a total length of about 10 mm.

The excess pressure in the measuring system and the pressure value inside the bubble in dependence of time is shown schematically in Fig. 3. As one can see, in the first stage of bubble formation the pressure inside the bubble is equal to that in the measuring system while the bubble radius decreases from r_0 to r. During the period of bubble growth from a radius r up to R at time $t = \tau_d$, the bubble pressure decreases quickly while the system pressure remains constant. Strictly speaking, the pressure p is equal to a certain constant value only when the volume of the measuring system V is infinitely large in comparison with the volume of a separating bubble v. In the present instrument the ratio v/V amounts to approximately 10^{-5} and thus, even in the period of fast bubble growth the pressure in the measuring system decreases only for about 1 Pa which is negligible in comparison with the value of excess pressure p = 1000–2000 Pa.

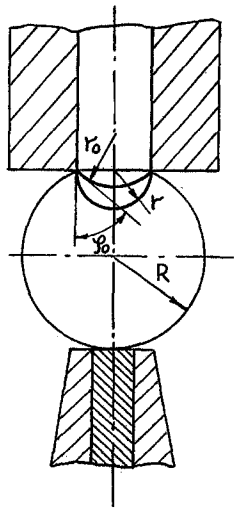

Fig. 2. Schematic of the bubble formation process at the tip of the capillary

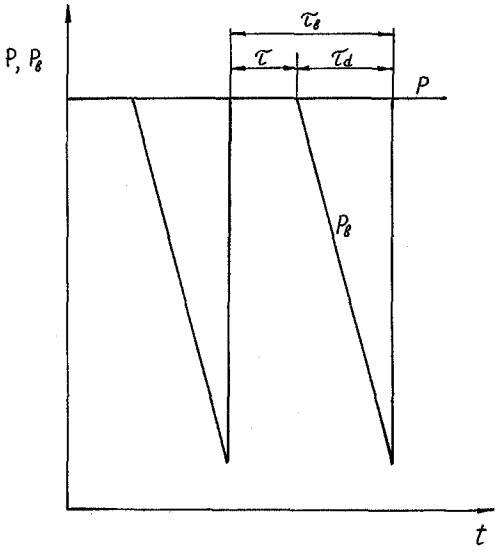

Fig. 3. The pressure change in the measuring system and in the bubble as a function of time

Except for the filling of the measuring system with the liquid under study all operations of the instrument are fully automated including the preparation steps:

- automatic air-tightness check;
- calibration of all sensors and transducers;
- performance of the measurement;
- interpretation and saving of data.

For starting the measuring run the necessary (maximum and minimum) air flow rates have to be set. After stabilization of all parameters the instrument measures the excess pressure in the system and the time interval between subsequent bubbles. The air flow rate is changed automatically by a given increment and the instrument repeats the measuring procedure until the limit is reached. The experimentally measured values, the pressure p in dependence of air flow rate L and time interval between subsequent bubbles τ_b, are registered and stored in the computer memory.

3. The theory for calculation of surface tension, surface lifetime and effective surface age

The value τ_d, the time interval necessary for the formation of a bubble with radius R, can be calculated under the conditions $p = \text{const}$ and $p_b = 2\sigma^*/R_i$ (where σ^* is the surface tension value and R_i is the actual value of the growing bubble) via the Poiseuille law [22, 24, 25]:

$$\tau_d = \frac{\tau_b L}{Kp}\left(1 + \frac{3r}{2R}\right), \tag{1}$$

where $K = \pi r^4/8l\eta$ is the Poiseuille law constant (for a non-immersed capillary Eq. (1) reads $L = Kp$), η is the gas viscosity and l is the capillary length. The calculation of τ_d can be simplified when taking into account the existence of two gas flow regimes for the gas flow leaving the capillary [10, 22, 25]: bubble flow regime when $\tau > 0$ and jet regime, when $\tau = 0$ and hence $\tau_b = \tau_d$. The dependence of p on L for some systems is presented in Fig. 4.

On the righthand side of the critical point the dependence of p on L is linear in accordance with the Poiseuille law. The existence of the electrode placed opposite the capillary controls the dimensions of bubbles. Under this condition $R = \text{const}$ at any given L in the region of the bubble flow regime [24]. Therefore, instead of Eq. (1) the following relation results [25]:

$$\tau_d = \tau_b \frac{Lp_c}{L_c p}, \tag{2}$$

where L_c and p_c are related to the critical point, and L and p are the actual values of the dependence left from the critical point.

The surface lifetime can be calculated via the formula derived in [25]:

$$\tau = \tau_b - \tau_d = \tau_b\left(1 - \frac{Lp_c}{L_c p}\right) \tag{3}$$

As one can see, Eq. (3) involves only experimentally available values. The critical point in the dependence p on L can easily be located. In the software the location is automatically calculated by an algorithm based on the Poiseulle law. To

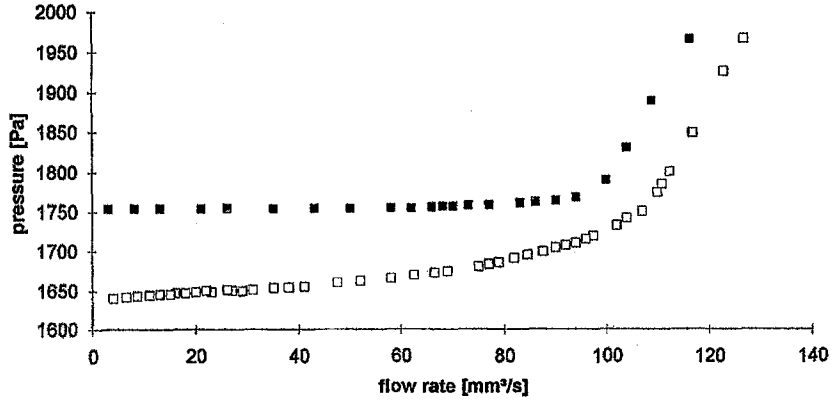

Fig. 4. Dependence of pressure p in the measuring system on air flow rate L, for the cases of water (■), and a water/glycerine mixture (ratio 2:3) (□) at 30 °C; $r = 0.0824$ mm

calculate the effective surface age (adsorption time) the following equation results [26, 29]:

$$\tau_a = \frac{\tau}{2\xi + 1}, \tag{4}$$

where $\xi = \sin\varphi_0/(1 + \sin\varphi_0)$ is the relative deformation rate of the bubble surface in the first stage of its growth, $\varphi_0 = \arccos(\sigma/\sigma_0)$ (Fig. 2), σ is the dynamic surface tension of the liquid at time τ, and σ_0 is surface tension of the liquid at $\tau = 0$ (usually equal to the surface tension of the pure solvent). The derivation of the relation for the relative surface deformation rate is based on the condition $p = \text{const}$ and Eq. (4) results from a model of convective diffusion of the surfactant to the deforming surface without considering the bubble displacement in the liquid. From Eq. (4) it follows that for values of σ not too close to σ_0 (for example, for aqueous solutions below 60 mN/m) ξ is approximately equal to 0.5, i.e., $\tau_a \approx \tau/2$. This coefficient is close to values obtained for other set-ups [3]. It is necessary to stress again the fact that Eq. (4) and also the expression for ξ are valid only for the case $p = \text{const}$, i.e., when the system volume V is large enough. If this condition is not fulfilled, as seems to be the case for the instruments described in [5, 11–15], the law for bubble surface change is unknown and it is impossible to obtain valid relations for ξ and τ_a. In these cases the physical pattern is absolutely different from that given in Fig. 2, so that in the initial moment the liquid meniscus can even have a convex form.

The surface tension value in the maximum bubble pressure method is calculated via the Laplace equation. As the capillary radius in the presented instrument is small, the deviation of the bubble shape from a spherical one can be neglected and need not to be considered by correction factors. Thus, the following equation results:

$$p = \frac{2\sigma}{r} + \rho g h + \Delta p, \tag{5}$$

where ρ is the density of the liquid, g is the acceleration of gravity, h is the depth the capillary is immersed into the liquid, and Δp is a correction value attributed to hydrodynamic effects. The use of the pressure value p in the measuring system instead of the pressure value in the bubble is caused by the equality of both in the first stage of bubble formation (Fig. 3). The existing difference can be attributed to some hydrodynamic effects:

1) aerodynamic resistance of the capillary during the passage of air, due to both the pressure change from p_b to p at the tip of the capillary and the displacement of the meniscus (Fig. 2) in the first stage of bubble formation (the radius grows from r_0 to r);
2) hydrodynamic resistance of liquid against the moving bubble.

The contribution of the first factor is negligible. An estimation of the second contribution was done using Stokes law for a viscous resistance of the liquid [22]. The correction value to the calculated surface tension value (that is, difference between measured value of dynamic surface tension and its real value) can be estimated according to the following relation:

$$\Delta\sigma = \frac{3}{2}\frac{\mu r}{\tau}, \tag{6}$$

where μ is the viscosity of the liquid.

Recent experimental studies [32] qualitatively corroborated the validity of Eq. (6): the value increases with increasing liquid viscosity, increasing capillary radius and decreasing surface lifetime. For liquids of small viscosity (water and aqueous surfactant solutions), the correction does not exceed the measurement error of $\pm$ 0.5 mN/m) even in the millisecond region of τ and it is allowed to exclude the correction parameter Δp from Eq. (5). For viscous liquids (in the region of 10–100 mm^2/s and more) the value can reach some mN/m (Fig. 4) at small τ. Therefore, to correct the resulting error, it is necessary to perform additional investigations with viscous model liquids (for example, water-glycerine solution) having the same viscosity as the liquid under test. Corrected (from influence of viscosity effects) values of dynamic surface tension can be obtained by subtracting the corresponding difference between apparent surface tension at the given bubble formation time and the equilibrium value at large bubble formation times obtained for the model liquid. Thus, using experimental values of p, L and τ_b, and via the determination of the critical point in the p vs. L dependence, it is possible to calculate the lifetime, effective surface age and dynamic surface tension of pure liquids and solutions according to formulae (3), (4)

and (6). In the present instrument all these steps are implemented as automatic procedures. After the measurement of a full set of experiments all obtained results can be stored on a harddisc or diskette or be printed out as tables and graphics.

4. The comparison with other methods

For comparison of the present maximum bubble pressure apparatus with other methods experiments with oscillating jet and inclined plate set-ups were performed. The detailed description of these methods were given elsewhere [33, 34]. Aqueous solutions of Triton X-100 (octylphenol polyglycol ether, $C_{14}H_{21}O(C_2H_4O)_{10}H$, Serva) of different concentrations (from 0.1 up to 5 g/l) were studied. The results, obtained with the help of all three mentioned methods, are presented in Figs. 5 and 6. As one can see, in all cases a very good agreement is obtained.

5. Examples of experimental results

Further studies of dynamic surface tensions of different systems were performed by using only the maximum bubble pressure method, the results of which are presented in Figs. 7–10. The dependence of dynamic surface tension of concentrated micellar solution of the non-ionic surfactant Triton X-100 at different temperature is shown in Fig. 7. The theory elaborated in [26, 29, 35] allows to calculate the micelle dissociation rate constant k from the initial linear section of the dependencies $\sigma(t^{-1})$ in Fig. 7. The obtained values for k (230–290 s^{-1}) independent of temperature give evidence about the entropy nature of the micelle dissociation process in Triton X-100 solutions.

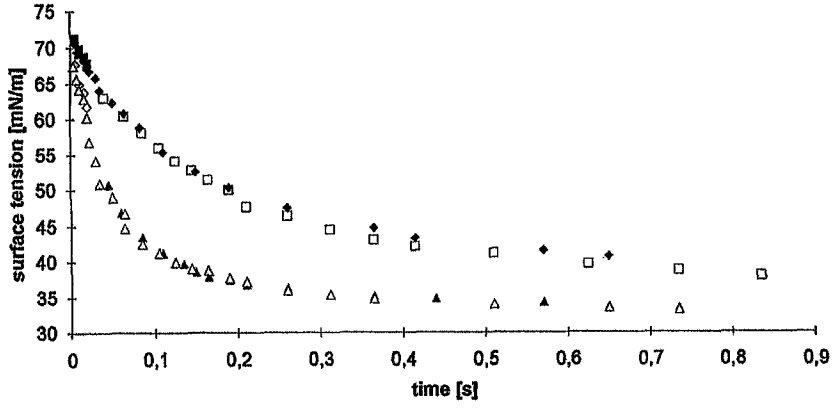

Fig. 5. Dynamic surface tension of Triton X-100 solutions, measured by the methods of oscillating jet (■ ◇), inclined plate (□ ▲) and maximum bubble pressure (◆ △) at concentration 0.2 (■ □ ◆) and 0.5 g/l (◇ △ ▲)

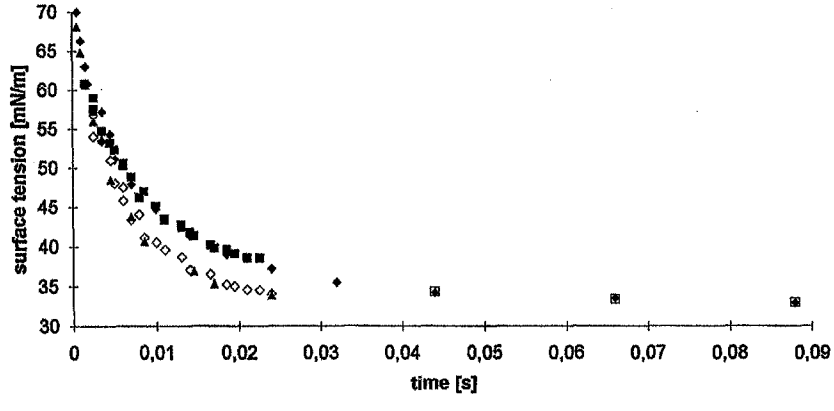

Fig. 6. Dynamic surface tension of Triton X-100 solutions, measured by the methods of oscillating jet (■ ◇), inclined plate (□) and maximum bubble pressure (◆ △) at concentration 2 (■ □ ◆) and 5 g/l (◇ △)

Results for micellar solutions of the anion-active sodium hexadecylsulphate at concentrations about 80 times higher than the CMC (CMC = 0.0006 mol/l) are given in Fig. 8. The calculated values of the micelle dissociation rate constant k show an increase with sodium hexadecylsulphate concentration. Especially at a concentration 40 times higher than the CMC a strong change in the k-values can be observed which is possibly connected with a change of the micelle shape.

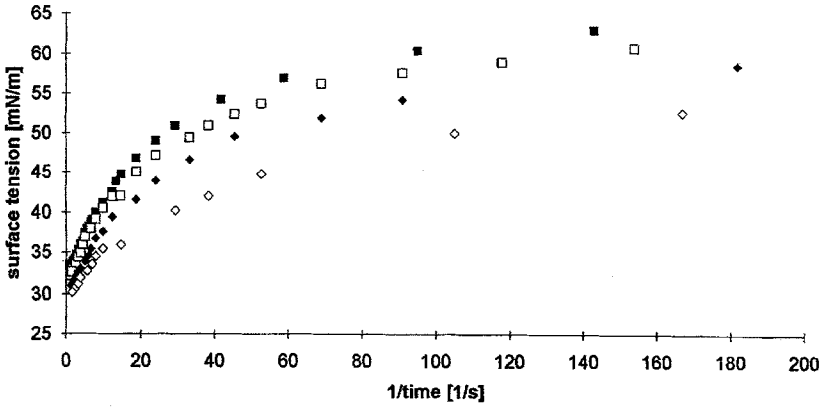

Fig. 7. Dynamic surface tension of a Triton X-100 solution at a concentration of 0.5 g/l (CMC = 0.1 g/l) at different temperature: 30 °C (■), 40 °C (□), 50 °C (◆) and 60 °C (◇)

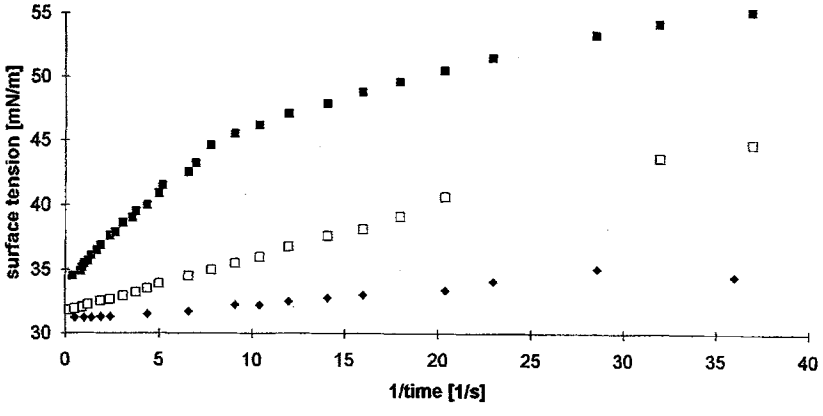

Fig. 8. Dynamic surface tension of a sodium hexadecylsulphate solution at different temperature: 40 °C (■), 60 °C (□) and 80 °C (◆), concentration 0.05 mol/l

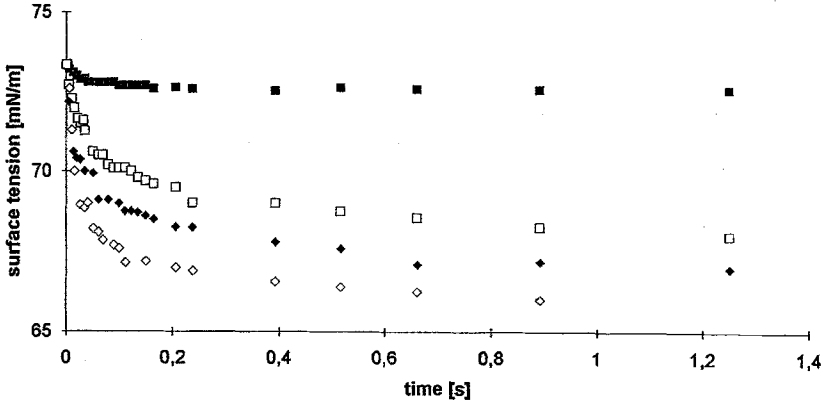

Fig. 9. Dynamic surface tension of water at 25 °C (■) and aqueous solutions of gelatine (10 g/l) at different temperature: 25 °C (□), 30 °C (◆) and 35 °C (◇); no correction of the viscosity effect

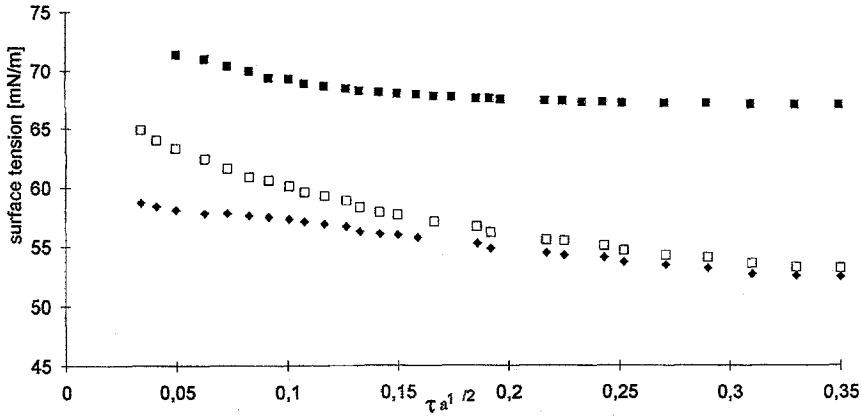

Fig. 10. Dynamic surface tension of a water/glycerine mixture (ratio 2:3) without (■) and with addition (□ ◆) of 0.002 mol/l sodium tetradecylsulphate; corrections taking into account the effect of viscosity (◆); temperature 30 °C

The dynamic surface tensions for water and aqueous gelatine solutions at different temperature are presented in Fig. 9. These results are not corrected with respect to the viscosity effect and therefore, the values at low bubble formation times could be somewhat too high. For pure water the correction value is negligible. In Fig. 10 the dynamic surface tension of sodium tetradecylsulphate (STS) in the viscous water-glycerine mixture (60% glycerine in water, $\mu = 8.5\ mm^2/s$) is displayed. For comparison the data for the same water-glycerine mixture without addition of the surfactant is shown in Fig. 10 and used for a "hydrodynamic correction". The results of correction for the present sodium tetradecylsulphate solution is also presented in Fig. 10. As discussed in [32] this correction is performed by subtracting the difference $\Delta\sigma = \sigma(\tau) - \sigma(\tau \rightarrow \infty)$, obtained for the surfactant-free solvent under the same conditions, from the obtained dynamic surface tension of the surfactant solution. These results satisfactorily correspond with diffusion theory.

6. Conclusion

The principle of the maximum pressure in bubbles formed at the tip of a capillary, which is immersed into a liquid, can be used for the exact and fast measurement of the dynamic surface tension. The developed theory of the method and the commercially available instrument including the necessary software allows to apply this method in practice. The presented experimental results show the high accuracy and good reproducibility of the measurements. The comparison of the dynamic surface tension data obtained from maximum bubble pressure experiments with the results from other methods yields excellent agreement. The method can be applied to different systems: aqueous and non-aqueous solutions of non-ionic and ionic surfactants (at low concentration as well as above CMC), protein solutions and other highly viscous liquids, different organic liquids and their solutions. The advantages of this new method are as follows:

- wide range of bubble surface lifetime (from 0.001 s up to 10 s, and in the commercial set-up MPT1 even up to 100 s and more);
- wide range of temperature control;
- easy handling of the automatically operating instrument, in preparation and measurement procedures, data processing and interpretation;
- control of the instrument via the serial port of any type of IBM-compatible computers.

Acknowledgements

The authors are very grateful to Dr. K.-H. Schano, Dr. G. Geeraerts, and Dr. A. Makievski for their help in performing the experiments, and to Mr. A. Zadov and Mr. A. Vertlyb, directors of the instrument-producing company EPRIZ (Donetsk, Ukraine), for the successful solution of a number of technical problems in the set-up of the maximum bubble pressure method. This work was supported by the Deutsche Forschungsgemeinschaft (grants 478/199/92 and 436 UKR). The support of the "Fonds der Chemischen Industrie" is also gratefully acknowledged (RM, 400429).

References

1. Rehbinder PA (1924) Phys Chem 111:447; (1927), Biochem Z 187:19
2. Adam NK, Shute HL, (1935) Trans Faraday Soc 31:204; (1938) 34:758
3. Kuffner RJ (1961) J Colloid Sci 16:797
4. Austin M, Bright BB, Simpson EA (1967) J Colloid Interface Sci 23:108
5. Bendure RL (1973) J Colloid Interface Sci 35:238
6. Finch JA, Smith GW (1973) J Colloid Interface Sci 45:81
7. Kragh AM (1964) Trans Faraday Soc 60:225
8. Kloubek J (1972) J Colloid Interface Sci 41:1
10. Kloubek J (1972) J Colloid Interface Sci 41:7
11. Razouk R, Walmsley D (1974) J Colloid Interface Sci 47:515
12. Miller TE, Meyer WC (1984) American Laboratory, February 91
13. Woolfrey SG, Banzon GM, Groves MJ (1986) J Colloid Interface Sci 112:583
14. Hua XY, Rosen MJ (1988) J Colloid Interface Sci 124:652
15. Mysels KJ, (1989) Langmuir 5:442
16. Tzykurina NN, Zadymova NM, Pugachevich PP, Rabinovich II, Markina ZN (1977) Koll Zh 39:513
17. Markina ZN, Zadymova NM, Bovkun OP (1987) Colloids Surf 22:9
18. Lunkenheimer K, Miller R, Becht J (1982) Colloid Polym Sci 260:1145
19. Lunkenheimer K, Hartenstein C, Miller R, Wantke KD (1984) Colloids Surf 8:271
20. Lunkenheimer K, Serrien G, Joos P (1990) J Colloid Interface Sci 134:407
21. Lin S-Y, McKeigue K, Maldarelli Ch (1991) Langmuir 7:1055
22. Fainerman VB (1979) Koll Zh 41:111
23. Fainerman VB, Lylyk SV (1982) Koll Zh 44:598
24. Fairnerman VB (1990) Koll Zh 52:921
25. Fainerman VB (1992) Colloids Surf 62:333
26. Makievski AV, Fainerman VB, Joos P, J Colloid Interface Sci (in press)
27. Joos P, Rillaerts (1981) J Colloid Interface Sci 79:96
28. Joos P, Fang JP, Serrien G (1992) J Colloid Interface Sci 151:144
29. FainermanVB, Makievski AV, Joos P (1993) J Phys Chem (Russia) 67:452
30. Garrett PR, Ward DR (1989) J Colloid Interface Sci 132:475
31. Van Hunsel J, Joos P (1987) Colloids Surf 24:139
32. Fainerman VB, Makievski AV, Miller R (1993) Colloids Surf 75:229
33. Van den Bogaert P, Joos P (1979) J Phys Chem 83:2244
34. Defay R, Petre G, In: Matijevic, Surface and Colloid Science, Vol 3. Wiley, New York, 1971, p 27

Received February 16, 1993;
accepted August 4, 1993

Authors' address:

Dr. R. Miller
Max-Planck-Institut
für Kolloid- und Grenzflächenforschung
Rudower Chaussee 5
12489 Berlin